

PAPER • OPEN ACCESS

Photocatalytic degradation of congo red using copper substituted cobalt ferrite

To cite this article: V S Kirankumar *et al* 2017 *IOP Conf. Ser.: Mater. Sci. Eng.* **263** 022027

View the [article online](#) for updates and enhancements.

Related content

- [Photocatalytic degradation of Reactive Black 5 and Malachite Green with ZnO and lanthanum doped nanoparticles](#)
N Kaneva, A Bojinova and K Papazova
- [Photocatalytic degradation of RhB and TNT and photocatalytic water splitting with CZTS microparticles](#)
S. S. Shinde
- [Strong Temperature Dependence of the Coercivity of \$\text{Pr}\(\text{Co}_{1-x}\text{Cu}_x\)_2\$ Compounds](#)
Hiroshi Maeda



IOP | ebooks™

Bringing you innovative digital publishing with leading voices to create your essential collection of books in STEM research.

Start exploring the collection - download the first chapter of every title for free.

Photocatalytic degradation of congo red using copper substituted cobalt ferrite

V S Kirankumar¹, B Hardik² and S Sumathi¹

¹School of Advanced Sciences, VIT University, Vellore - 632 014, Tamilnadu, India

²School of Mechanical Engineering, VIT University, Vellore – 632014, Tamilnadu, India

E-mail : sumathishanmugam2003@gmail.com

Abstract: $\text{Co}_{1-x}\text{Cu}_x\text{Fe}_2\text{O}_4$ nanoparticles with $x = 0$ and 0.5 were synthesized through the combustion method. The as-made materials are face centered-cubic close-packed spinel structures. The characterization techniques such as powder XRD, FTIR, UV-DRS and SEM studies collectively verified that the formed products are cobalt ferrite and copper substituted cobalt ferrite nanoparticles. In addition, the mean crystalline size, lattice parameter and band gap energy of nanoparticles are calculated. The photocatalytic activity of the obtained $\text{Co}_{1-x}\text{Cu}_x\text{Fe}_2\text{O}_4$ spinel nanoparticles is evaluated by monitoring the degradation of congo red under visible light irradiation.

1.Introduction

Manifestation of organic pollutants released from various industries such as textile, plastic, paper, cosmetics in water bodies is a major concern and a major threat to the environment and aquatic species [1, 2]. Research concerning the finding of new photocatalyst with high photocatalytic activity under visible light is focused intensively in order to solve this environmental problem. Semiconductor photocatalysts is one of the techniques used to reduce the organic pollutants present in water. Various methods such as adsorption, solvent extraction, floatation, adsorption and photocatalytic activity are reported [3-8]. Between the various methods, photocatalytic methodologies have been broadly considered for ecological decontamination after the revelation of high photocatalytic effectiveness of TiO_2 terminal in 1972 [9, 10].

Amongst the semiconductor spinel oxides, cobalt ferrite (CoFe_2O_4) is an outstanding magnetic material reported for an assortment of utilizations in biomedical, electronic and also in recording technology [11-13]. The magnetic character of the nanoparticles depends crucially on shape, size, purity and attractive stability [14, 15]. The structure of the spinel ferrite depends on the distribution of divalent ions (Co^{2+}) and trivalent ions (Fe^{3+}) in two different sites (octahedral and tetrahedral). Depends on the distribution of divalent ion and trivalent ions in the spinel it is called as normal (Divalent ions occupies tetrahedral sites) and inverse spinel (Divalent ion and half of the trivalent ion occupies octahedral sites and the remaining trivalent ion occupies tetrahedral sites) [16].

The replacement of cobalt ions in cobalt ferrite with various divalent ions leads to distinguished properties and interesting applications. Substitutions of different cations in cobalt ferrite have examined to enhance the physic-chemical properties [17, 18]. Recently copper substituted cobalt ferrite is reported for



its enhanced antibacterial properties [19]. Copper ferrite, cobalt ferrite is described for its photocatalytic activity for the degradation of the dyes [20, 21]. Copper substituted cobalt ferrite is not reported for its photocatalytic activity. This inspires us to carry out the synthesis of cobalt ferrite and copper substituted cobalt ferrite and its photocatalytic activity for the degradation of congo red under visible light irradiations.

2. Materials and methods

2.1 Materials

Cobalt nitrate (s.d fine 97.0%), copper nitrate (s d fine 99.0%), ferric nitrate (s d fine 98.0%), glycine (s.d fine 99.5%), congo red (s.d fine 98.0%) and hydrogen peroxide solution (s d fine 30%).

2.2 Solution combustion method

Cobalt ferrite, copper substituted cobalt ferrite ($\text{Co}_{1-x}\text{Cu}_x\text{Fe}_2\text{O}_4$ $x = 0, 0.5$) were prepared by solution combustion method. Stoichiometric quantities of the reactants were weighed and dissolved in double distilled water. Then known quantity of glycine was added as a fuel to the mixed precursors. The contents in the beaker were concentrated on a hot plate for 10 min. After that the concentrated solution was kept in the preheated muffle furnace (500 °C). The powder was ground well and calcined at 700 °C for 2 h.

2.3 Characterization

The nanoparticles were characterized by powder X-ray diffraction (XRD) in the 2 theta range 10-70° using D8 advance BRUKER instrument. FT-IR spectrophotometer (SHIMADZU model) was used to identify the characteristic functional groups in the synthesized compounds. Diffuse reflectance spectroscopy (DRS) (JASCO-V670 spectrophotometer) was used to study the optical properties of the compounds. ZESIS EVO18 instrument was used to study the surface morphology (SEM-EDAX) of the synthesized compounds.

2.4 Photocatalytic activity

The photocatalytic activity of $\text{Co}_{1-x}\text{Cu}_x\text{Fe}_2\text{O}_4$ ($x = 0, 0.5$) nanoparticles were assessed by the photodegradation of congo red (10 ppm) in visible light (tungsten 500W). Initially, 10 mg of the compound was added into 50 ml of dye solution. Additionally, 50 μl of hydrogen peroxide (oxidizing agent) was added into the mixture solution. In order to attain the adsorption/desorption equilibrium, the solution was stirred for 60 minutes in dark condition. After the irradiation, in regular intervals of time 3 ml of the sample were taken out and centrifuged to discard the photocatalyst particles. The filtrate was analyzed using UV-visible spectrophotometer. Degradation efficiency was calculated using the following equation.

$$\% \text{ degradation} = \frac{C_0 - C_t}{C_0} \times 100 \quad (1)$$

Here, C_t - the concentration of dye solution at time t and C_0 - initial concentration of dye solution .

3. Results and discussion

3.1 Phase identification

Fig. 1 depicts the powder XRD pattern of $\text{Co}_{1-x}\text{Cu}_x\text{Fe}_2\text{O}_4$ $x = 0, 0.5$ nanoparticles. All the diffraction peaks can be indexed very well to the standard cubic phase of cobalt ferrite according as JCPDS No. 96-591-0064. The pattern indicates that the synthesized compounds were pure without any impurities [19]. FT-IR spectra of the synthesized compounds are given in Fig. 2. Two absorption bands at 530 (ν_1) and 420 (ν_2) are characteristic modes of spinel ferrites. A broad absorption peak was observed from 530 to

525 cm^{-1} which can be ascribed to the intrinsic vibrations of tetrahedral complex. Another peak appeared at the 428 to 421 cm^{-1} which could be attributed to the octahedral complex [22].

The shape and morphology of the cobalt ferrite and copper doped cobalt ferrite nanoparticles are examined by SEM-EDAX which is shown in Fig. 3. The morphology reveals that the samples consist of agglomerated nanoparticles. Due to the release of the large amount of gases during synthesis, the large pores can be visualized in the SEM images. In addition, the elemental composition was analyzed using EDAX. It shows that the nanoparticles are composed of Cu, Co, Fe and O in copper substituted cobalt ferrite and Co, Fe and O in cobalt ferrite without any additional impurities.

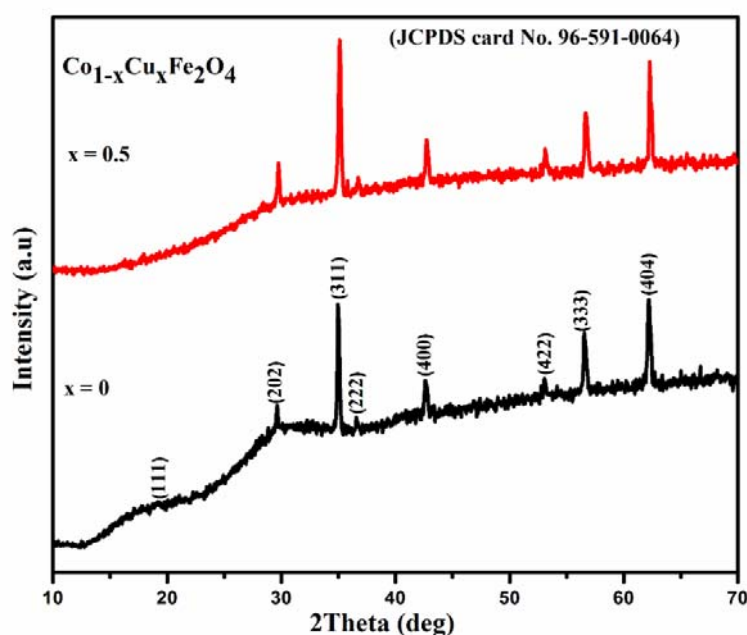


Figure 1. Powder XRD pattern of $\text{Co}_{1-x}\text{Cu}_x\text{Fe}_2\text{O}_4$ $x = 0, 0.5$ nanoparticles

For a semiconductor like spinels, the band gap value is significant because of its electrical and optical properties in various applications (e.g photovoltaic devices or photocatalysis). It was established that the optical properties, such as band gap energy vary with the synthesis parameters and substitution [23]. The optical band gap (E_g) is calculated from the Tauc's relation [24]. Fig. 4 shows the graphs of $(\alpha/h\nu)^2$ versus $h\nu$, where α – absorption coefficient of the cobalt ferrite and copper doped cobalt ferrite at a certain value of wavelength λ , h – planck's constant, and ν – the frequency of light. The band gap values of ferrite nanoparticles are shown in Fig. 4. Copper substitution in cobalt ferrite decreased the band gap from 1.46 to 1.24 eV. Therefore, the copper substituted cobalt ferrite is expected to have improved photocatalytic activity.

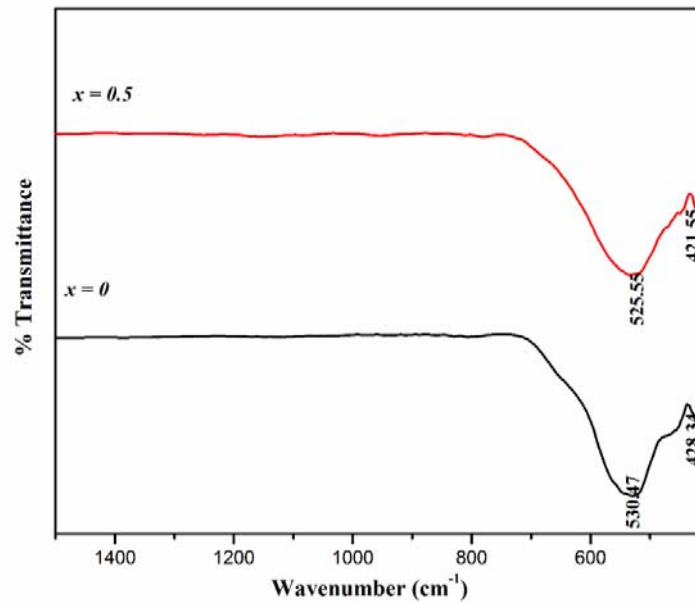


Figure 2. FTIR spectra of $\text{Co}_{1-x}\text{Cu}_x\text{Fe}_2\text{O}_4$ $x = 0, 0.5$ nanoparticles

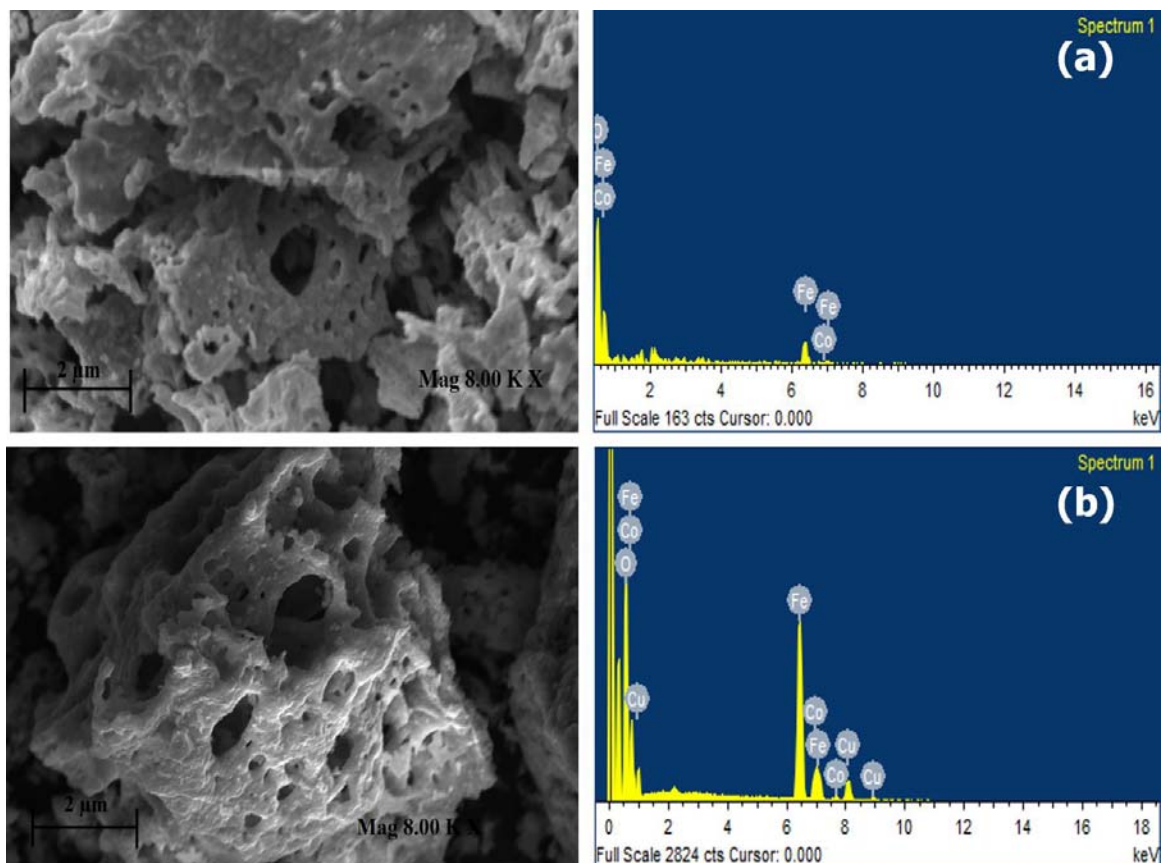


Figure 3. SEM-EDAX of $\text{Co}_{1-x}\text{Cu}_x\text{Fe}_2\text{O}_4$ (a) $x = 0$, (b) $x = 0.5$ nanoparticles

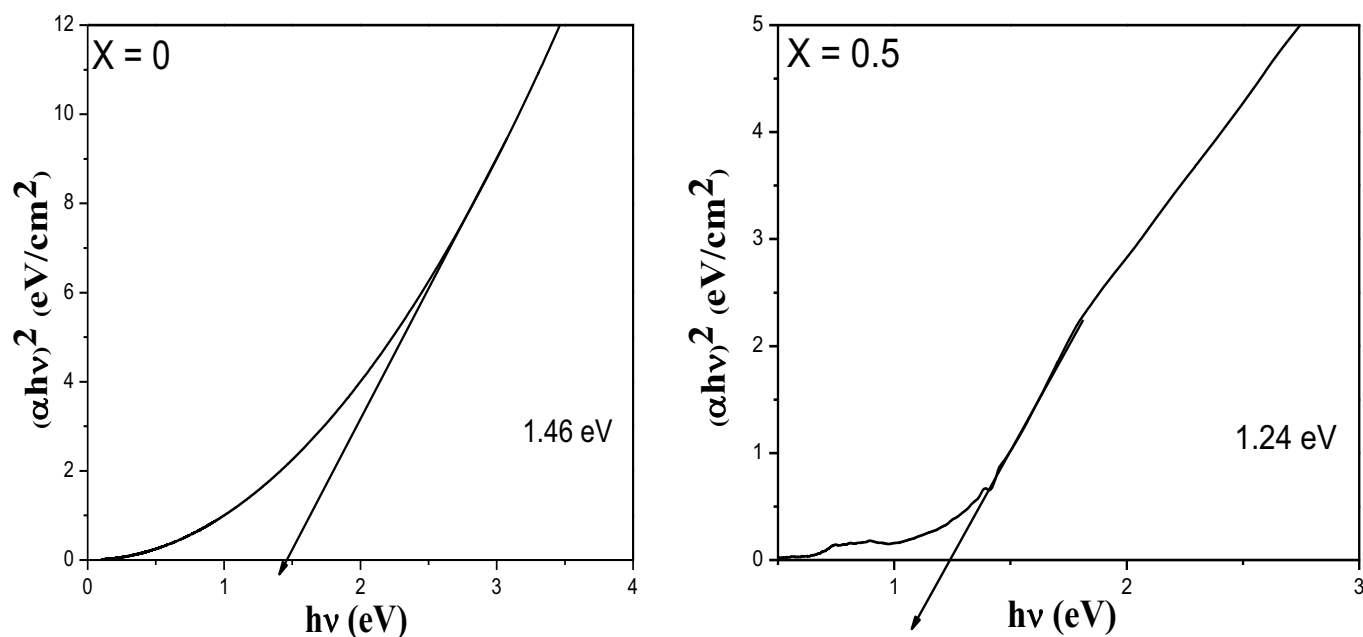


Figure 4. Band gap energy of $\text{Co}_{1-x}\text{Cu}_x\text{Fe}_2\text{O}_4$ (a) $x = 0$, (b) $x = 0.5$ nanoparticles

3.2 Photocatalytic activity

CR shows the maximum absorption at 492 nm. The degradation of dye is noted from the decrease in the absorption maximum of congo red dye at regular time intervals of every 30 min. As an initial study, the activity of the synthesized catalysts was checked with 10 mg of the catalyst under visible light for 90 minutes. 50 μl of the hydrogen peroxide was used as the oxidizing agent to improve the quantum yield of hydroxyl radical [25]. Because the photo catalytic activity mechanism mainly depends on the formation of $\cdot\text{O}_2^-$ (super oxide anion radical) and $\cdot\text{OH}$ (hydroxyl) radicals which are generated through the photo excitation of electrons from valence and conduction band. Fig. 5 shows the absorbance of Congo red (CR) dye solution at various time intervals in the presence of copper substituted cobalt ferrite photocatalyst under visible light irradiation. The percentage of photocatalytic degradation [26] of CR by cobalt ferrite and copper substituted cobalt ferrite nanoparticles are given in Fig. 6. Copper substitution in cobalt ferrite (71.23%) enhanced the photodegradation of cobalt ferrite (69.24%) slightly. Huang et. al. reported 85% degradation of CR under visible light in 390 min using $\text{Nb}_2\text{O}_5/\text{ZnAl-LDH}$ composites [27]. Miao et. al. conveyed 97.91% degradation of CR in 20 min using 25 mg of the RGO/PANI/ Cu_2O composite hydrogel catalyst [28]. Further research is required on the quantity of the catalyst, dye concentration, hydrogen peroxide concentration and source of irradiation.

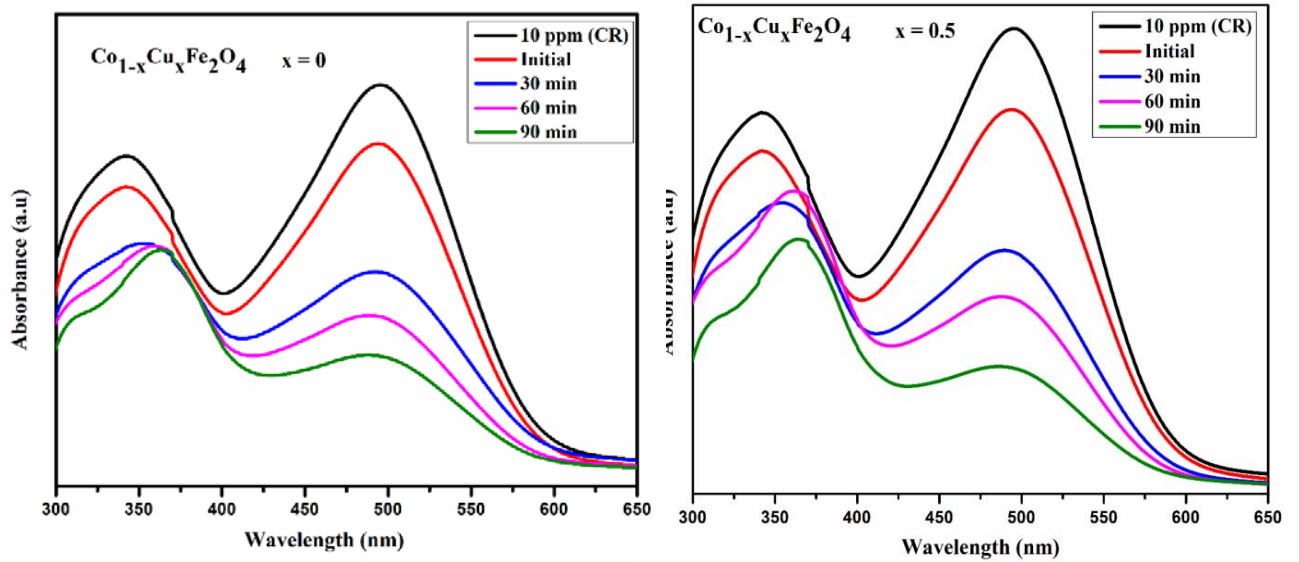


Figure 5. UV-Visible absorbance spectrum of CR using $\text{Co}_{1-x}\text{Cu}_x\text{Fe}_2\text{O}_4$ $x = 0, 0.5$ nanoparticles

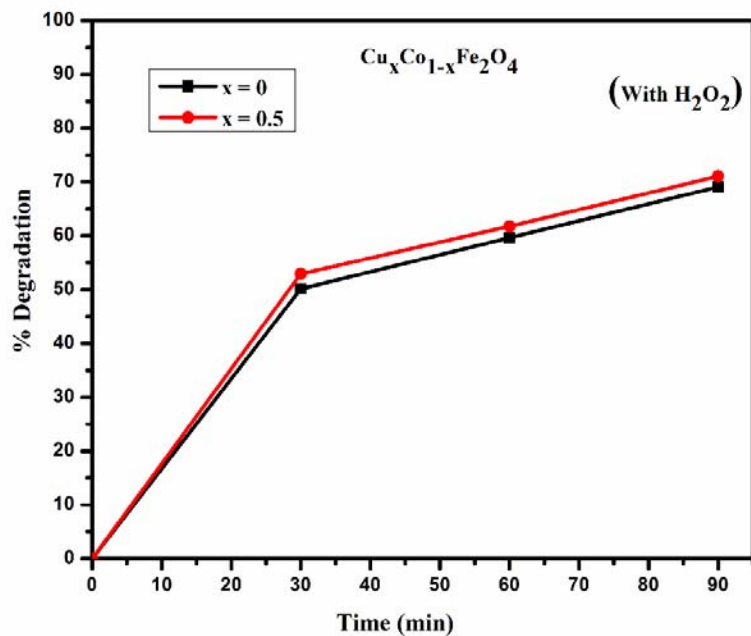


Figure 6. The degradation of CR using $\text{Co}_{1-x}\text{Cu}_x\text{Fe}_2\text{O}_4$ $x = 0, 0.5$ nanoparticles

4. Conclusion

To conclude, the substitution of copper into cobalt ferrite spinel structure showed a positive effect on photocatalytic degradation process. Cobalt ferrite and copper substituted cobalt ferrite were manufactured by combustion method. The ferrite nanoparticles were analyzed by several experimental techniques. Copper substituted cobalt ferrite nanoparticles exhibits low band gap energy of 1.24 eV. Photocatalytic study reveals that copper substituted cobalt ferrite nanoparticles can effectively degrade congo red than cobalt ferrite nanoparticles. The degradation of the congo red can reach 71.37% in 90 min using copper substituted cobalt ferrite nanoparticles.

Acknowledgement

The financial support from the VIT Seed grant for research for this work is greatly appreciated.

References

- [1] Wang X W, Tian H W, Yang Y, Wang H, Wang S M, Zheng W T and Liu Y C 2012 *J. Alloy. Comp.* **524**, 5-12
- [2] Schwarzenbach R P, Escher B I, Fenner K, Hofstetter T B, Johnson C A, Gunten U and Wehrli 2006 *Science* **313**, 1072-1077
- [3] Lu D B, Zhang Y, Lin S X and Wang L T 2013 *J. Alloy. Comp.* **579**, 336-342
- [4] Ghoreishi S M and Haghghi R 2003 *Chem. Eng. J.* **95**, 163-169
- [5] Lee D W, Hong W H and Hwang K Y 2000 *Sep. Sci. Technol.* **35**, 1951-1962
- [6] Wu J N, Eiteman M A and Law S E 1998 *J. Environ. Eng.* **124**, 272-277
- [7] Gary V K, Yadav A B and Kumar R 2003 *Bioresour. Technol.* **89**, 121-124
- [8] Kabil M A and Ghazy S E 1994 *Sep. Sci. Technol.* **29**, 2533-2539
- [9] Fujishima A and Honda K 1972 *Nature* **238**, 37-38
- [10] Wang Y G, Li B, Zhang C L, Cui L F, Kang S F, Li X and Zhou L H 2013 *Appl. Catal. B* **131**, 277-284
- [11] Gao X, Liu L, Birajdar B, Ziese M, Lee G, Alexe M and Hesse D 2009 *Adv. Funct. Mater.* **19**, 3450-3455
- [12] Ahalya K, Suriyanarayanan N and Ranjithkumar V 2014 *J. Magn. Magn. Mater.* **372**, 208-213
- [13] Bensebaa F, Zavaliche F, Ecuyer P L, Cochrane R W and Veres T 2004 *J. Colloid Inter.Sci.* **277**, 104-110
- [14] Maaz K, Karim S, Mumtaz A, Hasanain S K, Liu J and Duan J L 2009 *J. Magn. Magn. Mater.* **321**, 1838-1842
- [15] Kumar A, Yadav N, Rana D S, Kumar P, Arora M and Pant R.P 2015 *J. Magn. Magn. Mater.* **394**, 379-384
- [16] Goldman A 2006 *Modern Ferrite Technology, 2nd edn. Springer, Pittsburgh*
- [17] Mane D, Birajdar D, Patil S, Shirsath S E and Kadam R 2011 *J. Sol-Gel Sci. Tech.* **58**, 70
- [18] Aghav P, Dhage V N, Mane M L, Shengule D, Dorik R and Jadhav K 2011 *Physica B.* **406**, 4350
- [19] Samavati A, Mustafa M K, Ismail A F, Othman M H D and Rahman M A 2016 *Mater. Express*, **6**, 473-482
- [20] Nasiri A, Nasiri M, Nouhi S and Khodadadia S 2017 *J. Mater. Sci: Mater. Electron* **28**, 2401-2406
- [21] Mishra D, Kamal Senapati K, Borgohain C and Perumal A 2012 *J. Nanotech.* Article ID 323145, 6 pages
- [22] Kiran V S and Sumathi S 2017 *J. Magn. Magn. Mater.* **421**, 113-119
- [23] Das N S, Ghosh P K, Mitra M K and Chattopadhyay K K 2010 *Phys. E* **42**, 2097-2102

- [24] Varshney D, Sharma P, Satapathy S and Gupta P K 2014 *J. Alloy. Compd.* **584** 232-239
- [25] Ejhieh A N and Moeinirad S 2011 *Desalination* **273** 248-257
- [26] Kirankumar V S and Sumathi S 2017 *Mat. Res. Bull.* **93** 74–82
- [27] Huang G, Chen J, Wang D, Sun Y, Jiang L, Yu Y, Zhou J, Mab S and Kang Y 2016 *Mat. Lett.* **173**, 227–230
- [28] Miao J, Xie A, Li S, Huang F, Cao J and Shen Y 2016 *Appl. Sur. Sci.* **360**, 594–600